Biochemical Pharmacology, Vol. 51, pp. 103–115, 1996.
Copyright © 1995 Elsevier Science Inc.

ISSN 0006-2952/96/$15.00 + 0.00
SSDI 0006-2952(95)02109-4

N,N′-Bis-(3,4,5-trimethoxybenzyl) Ethylenediamine N,N′-diacetic Acid as a New Iron Chelator with Potential Medicinal Applications against Oxidative Stress

Jean-Baptiste Galey, Jacqueline Dumats, Sylvie Genard, Odile Destree, Patrick Pichaud, Philippe Cctroux, Laurent Marrot, Iréna Beck, Bona Fernandez, Gilles Barre, Michel Seite, Georges Hussler and Michel Hocquaux*

L'ORÉAL RESEARCH CENTER, 1 AVENUE EUGÈNE SCHUELLER, 93600 AULNAY SOUS BOIS, FRANCE

ABSTRACT. N,N′-bis-(3,4,5-trimethoxybenzyl) ethylenediamine N,N′-diacetic acid dihydrochloride (OR10141) is a member of a recently described series of "oxidative stress activatable iron chelators." These chelators have a relatively low affinity for iron but can be site-specifically oxidized, in situations mimicking oxidative stress *in vitro*, into species with strong iron-binding capacity. It is hoped that this local activation process will minimise toxicity compared to strong iron chelators that may interfere with iron metabolism. The present paper describes the results of experiments aimed at characterising oxidative reactions between iron-OR10141 complexes and hydrogen peroxide. Incubation of ascorbate and hydrogen peroxide with the ferric chelate of OR10141 in neutral aqueous solution yields a purple solution with a chromophore at 560 nm, which is consistent with an o-hydroxylation of one of the trimethoxybenzyl rings. Oxidation of OR10141 also takes place, although more slowly, by incubating hydrogen peroxide with ferric OR10141 complex in the absence of reductant. HPLC analysis shows that OR10141 is consumed during the reaction and transformed principally into N-(2-hydroxy 3,4,5-trimethoxybenzyl) N′-(3,4,5-trimethoxybenzyl) ethylenediamine N,N′-diacetic acid. Minor products are also formed, some of which were identified by mass spectrometry. The protective effect of OR10141 *in vitro* against DNA single strand breaks, protein damage, and lipid peroxidation induced by Fenton chemistry suggests that this compound is able to compete for iron with biological molecules and, thus, that this strategy of protection against oxidative stress is feasible. In addition, preliminary results showing protective effects of OR10141 dimethyl ester against toxicity induced by hydrogen peroxide in cell culture are described. It is concluded that OR10141 and related prodrugs might be useful *in vivo* in chronic situations involving oxidative stress. BIOCHEM PHARMACOL 51;2:103–115, 1996.

KEY WORDS. oxidative stress; iron chelator; hydroxyl radical; site specific reaction; intramolecular hydroxylation; hydrogen peroxide

Cellular damage induced by radical-mediated oxidations has been implicated in many pathological conditions, such as ischemia reperfusion injury, inflammation, neurodegenerative disease, cancer, and also in the aging process (see, for instance [1–6]). During oxidative insults, both cell structure and function may be dramatically affected, involving DNA strand breakage, lipid peroxidation, damage to proteins, and a rise in intracellular calcium leading to activation of proteases and nucleases. Both enzymatic and nonenzymatic antioxidant systems provide a highly efficient protection for living organisms against oxidative stress [7]. Effective sequestration of iron is one of the most important natural antioxidant defenses [8–10]. Hence, iron is never "free" in biological systems but carefully handled by transport and storage proteins, such as transferrin and ferritin, that prevent reactions between iron and oxygen or hydrogen peroxide and, therefore, prevent the formation of harmful radical species. On the other hand, traces of redox active metal ions, especially iron, are thought to be released from their normal sites during oxidative stress and then to participate in Fenton chemistry [11–12]. Most damage done by superoxide and hydrogen peroxide is, indeed, thought to be linked to their conversion into hydroxyl radicals ($HO^{\cdot}$) by iron-catalysed site-specific reactions [8, 13, 14].

The use of strong iron chelators is, therefore, a potential strategy of protection against oxidative damage. Hence, much *in vitro* work has shown the ability of iron chelators to protect cells against oxidative injury (see, for instance [15–19]). Iron-

* Corresponding author. Tel. (33) 1 48 68 94 58 FAX (33) 1 48 68 94 89.

† *Abbreviations:* HBED, N,N′-bis-(2-hydroxybenzyl) ethylenediamine N,N′-diacetic acid; DCI, desorption chemical ionization; MS, mass spectrometry; ESI, electro spray ionization; DMF, N,N-dimethylformamide; G-6-PDH, glucose-6-phosphate dehydrogenase; MOPS, 3-morpholino-propane sulfonic acid; TCA, trichloroacetic acid; TBA, 2-thiobarbituric acid; DMEM, Dulbecco's minimal essential medium; HBBED, N-(2-hydroxybenzyl) N′-benzyl ethylenediamine N,N′-diacetic acid; DBED, N,N′-bis-benzyl ethylenediamine N,N′-diacetic acid; HCHD, hydroxy cyclohexadienyl radical; EDDA, ethylenediamine N,N′-diacetic acid; DF, deferoxamine; TBARs, thiobarbituric acid reactive substances; CHO, Chinese hamster ovary cells.

Received 19 April 1995; accepted 1 September 1995.

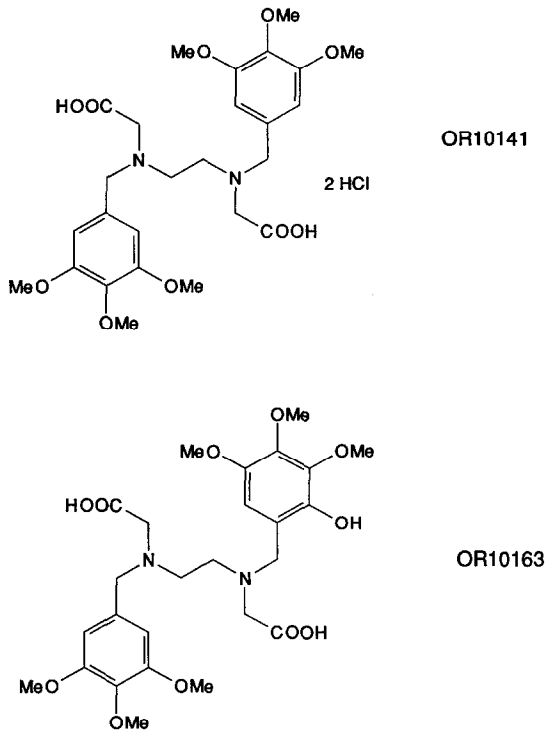

FIG 1. Structures of OR10141: N,N′-bis-(3,4,5-trimethoxybenzyl) ethylenediamine N,N′-diacetic acid and of its monohydroxylation product: N-(2-hydroxy 3,4,5-trimethyoxybenzyl) N′-(3,4,5-trimethoxybenzyl) ethylenediamine N,N′-diacetic acid (OR10163).

chelating agents may avert oxidative damage by preventing Fe(III) reduction or Fe(II) reaction with O_2, $O_2^{-\cdot}$, and H_2O_2. This may be achieved by altering the redox potential of iron or by suppressing its accessibility to superoxide and/or hydrogen peroxide [20, 21]. The chelator may also direct $HO^{\cdot}$ damage to itself, thereby sparing more important targets that bind iron, such as DNA.

There have been few *in vivo* studies with iron-chelating drugs in non-iron-overload situations (see [22] and references cited therein), probably because strong iron chelators are likely, owing to the ubiquitous role of iron in cell functions, to provoke adverse effects when used for prolonged periods of time by removing "safe" metals from various sites [23–25].

We have recently described a new series of scavenging chelators [26] that can be site-specifically oxidised by intramolecular hydroxylation into species bearing a phenolate moiety able to coordinate iron. The resulting chelates have an increased association constant and show a decrease in reactivity *versus* reduced oxygen species. They can be looked upon as "oxidative stress activatable iron chelators."

N,N′-bis-(3,4,5-trimethoxybenzyl)ethylenediamineN,N′-diacetic acid dihydrochloride (OR10141, Fig. 1) was selected in the series because electrophilic addition of $HO^{\cdot}$ to the aromatic ring is favoured by the increased electron density due to methoxy substituents, thereby promoting the reaction mechanism described in Fig. 2.

We report here the results of experiments designed to investigate the mechanism of the oxidative reaction between iron OR10141 complexes and hydrogen peroxide. In addition, we describe protective effects of OR10141 against DNA single strand breakage, lipid peroxidation, and protein damage *in vitro* and against toxicity induced by hydrogen peroxide in cell culture.

MATERIALS AND METHODS

Material

Sodium ascorbate, ferrous ammonium sulfate, potassium nitrate, bromoacetic acid, EDDA and TBA were purchased from Fluka. Ferric chloride (hexahydrate), hydrogen peroxide, EDTA tetrasodium salt, chelex resin, trichloroacetic acid, DF mesylate, glucose oxydase, and o-phenantroline were purchased from Sigma, 3,4,5-trimethoxybenzaldehyde, ethylenediamine, and sodium borohydride from Aldrich, HBED from Strem. Bidistilled water for injection (Biosedra, France) was used in the experiments. Other solvents were of the highest purity available and were used without further purification.

Rat liver microsomes were obtained from Iffa Credo (Lyon, France).

UV visible spectra were recorded with a Perkin Elmer Lambda 2S spectrophotometer. HPLC analysis was performed with a Waters Model 510 pump equipped with a Waters 990 photodiode array detector. The MS were obtained either by DCI or electron impact ionization (EI) with a Finnigan Mat SSQ 710 mass spectrometer or by HPLC/MS with a Fisons Platform mass spectrometer equipped with an atmospheric pressure ion source in the ESI mode. In both techniques, positive ion detection was used.

Proton and ^{13}C NMR analyses were performed with a Bruker AMX 500 spectrometer.

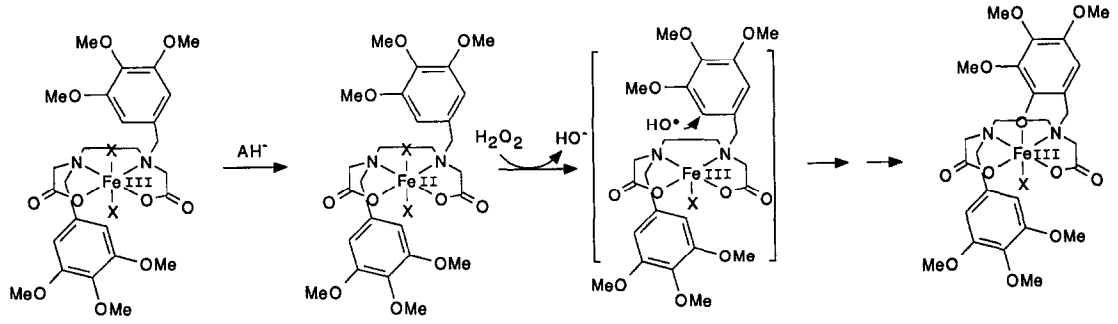

FIG. 2. Proposed reaction scheme between Fe(II)-OR10141 and H_2O_2 (X represents axial ligands).

TABLE 1. Mass spectrometry (MS) and nuclear magnetic resonance (NMR) data permitting identification of compound 1 as N-(2-hydroxy 3,4,5-trimethoxybenzyl) N'-(3,4,5-trimethoxybenzyl) ethylenediamine N,N'-diacetic acid (OR10163)

^{1}H NMR parameters (δ, ppm) of 1 iron chelate in D_2O in the presence of $Na_2S_2O_4$.	3.40 (t, 2H); 3.44 (t, 2H); 3.62 (s, 2H); 3.66 (s, 2H); 3.68 (s, 3H); 3.72 (s, 3H); 3.75 (s, 3H); 3.78 (s, 6H); 4.14 (s, 2H); 4.20 (s, 2H); 6.75 (s, 1H); 6.76 (s, 2H)
^{13}C NMR parameters (δ, ppm) of 1 iron chelate in D_2O in the presence of $Na_2S_2O_4$	47.43; 47.55; 51.55; 53.50; 56.62; 105.35; 108.44; 108.81; 124.14; 134.95; 135.45; 138.53; 140.72; 140.86; 143.37; 149.77; 150.14; 150.81; 168.48
ESI/MS (loop injection) of 1 iron chelate m/z (% relative abundance)	628 (100), $[M + Na]^+$ 606 (90), $[M + H]^+$ 181 (90), $[(MeO)_3 - C_7H_4]^+$
HPLC/ESI/MS of compound 1 m/z (% relative abundance)	575 (30), $[M + Na]^+$ 553 (100), $[M + H]^+$

^{1}H and ^{13}C and NMR analysis were performed on compound 1 as ferric iron chelate in D_2O in the presence of sodium dithionite ($Na_2S_2O_4$) as described in Materials and Methods. Sodium dithionite was added directly to the NMR tube sample to reduce paramagnetic high-spin ferric iron to diamagnetic ferrous iron and to allow restitution of fine structure.

MS analysis of 1 was done both on isolated iron chelate and on ligand as described in Materials and Methods.

SYNTHESIS OF OR10141. OR10141 was synthesised by adaptation of reported procedures [27].

N,N'-BIS-(3,4,5-TRIMETHOXYBENZYLIDENE)ETHYLENEDIAMINE. 50.0 g (255 mmoles) of 3,4,5-trimethoxybenzaldehyde was dissolved in 300 mL of methanol, to which 8.50 mL (127.5 mmoles) of ethylenediamine was added. The reaction mixture was stirred for 1 hr at room temperature and then cooled at 5°C. The yellow crystalline Schiff base was collected by filtration and washed extensively with cold methanol to yield 49.4 g (93%) of N,N'-bis-(3,4,5-trimethoxybenzylidene) ethylenediamine as a cristalline powder m.p. = 148°C.

^{1}H NMR (in d^6 DMSO): δ (ppm) = 3.70 (s, 6H), 3.80 (s, 12H), 3.85 (s, 4H), 7.04 (s, 4H), 8.26 (s, 2H).

MS (EI): m/z: 416, $[M^+]$

Anal. Calcd. for $C_{22}H_{28}N_2O_6$: C, 63.45; H, 6.78; N, 6.73; O, 23.05. Found: C, 63.47; H, 6.75; N, 6.74; O, 23.19.

N,N'-BIS-(3,4,5-TRIMETHOXYBENZYL) ETHYLENEDIAMINE DIHYDROCHLORIDE. 20.0 g (48.0 mmoles) of N,N'-bis-(3,4,5-trimethoxybenzylidene) ethylenediamine was suspended in 400 mL ethanol to which 2.27 g (60 mmoles) of $NaBH_4$ was added portionwise. The reaction mixture was stirred at 55–60°C for 2 hr and then allowed to stand at room temperature for 1 hr. 30 mL of 6N HCl were then slowly added to adjust the pH of the solution to 1. The crystalline dihydrochloride was collected by filtration, washed with cold ethanol, and vacuum dried over P_2O_5 to yield 19.5 g of N,N'-bis-(3,4,5-trimethoxybenzyl) ethylenediamine dihydrochloride.

^{1}H NMR (in d^6 DMSO): δ (ppm) = 3.37 (s, 4H), 3.67 (s, 6H), 3.81 (s, 12H), 4.13 (s, 4H), 7.01 (s, 4H), 9.89 (s, 4H).

MS (EI): m/z: 420, $[M^+]$, 181, $[(MeO)_3\text{-}C_7H_4]^+$.

Elementary analysis showed the presence of NaCl, but the product was used without further purification for the following steps.

N,N'-BIS-(3,4,5-TRIMETHOXYBENZYL)ETHYLENEDIAMINE N,N'-DIACETIC ACID DIHYDROCHLORIDE (OR10141). 14.0 g (28.4 mmoles) of N,N'-bis-(3,4,5-trimethoxybenzyl) ethylenediamine dihydrochloride was dissolved in 140 mL of water containing 7.50 mL of 30% sodium hydroxide. Bromoacetic acid, 7.88 g (56.8 mmoles), was dissolved in 16 mL water in an ice-water bath. 4.76 g of $NaHCO_3$ was added to this solution portionwise. The two solutions were mixed and the reaction mixture heated to 40°C. NaOH (30% solution) was used to maintain the pH of the solution in the range of 10–11 for 4 hr. The reaction mixture was then allowed to stand at room temperature overnight. Concentrated HCl was added to the reaction solution until pH was reduced to 2. The white precipitate was filtered and recrystallised from ethanol/water 1:1 to yield 10.6 g (60%) of N,N'-bis-(3,4,5-trimethoxybenzyl) ethylenediamine N,N'-diacetic acid dihydrochloride as a white powder m.p. = 205°C.

^{1}H NMR (in d^6 DMSO): δ (ppm) = 2.82 (s, 4H), 3.27 (s, 4H),

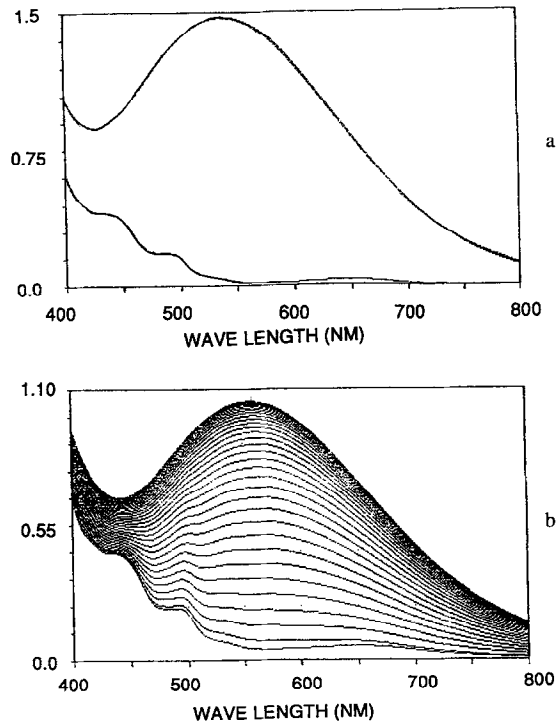

FIG. 3. (A) Visible spectrum in 50 mM acetate buffer pH 5.4 of 1 mM Fe(III) OR10141 to which was added 10 mM ascorbate and 10 mM hydrogen peroxide; incubation time was 5 min at 25°C. (B) Evolution of visible spectrum of Fe(III) OR10141 (0.8 mM) in 50 mM acetate buffer pH 5.4 after addition of hydrogen peroxide at a final concentration of 10 mM. One spectrum was recorded every minute at 25°C.

3.63 (s, 6H), 3.71 (s, 12H), 3.74 (s, 4H), 6.64 (s, 4H).
MS (EI): m/z: 537, $[M + H]^+$; 181, $[(MeO)_3\text{-}C_7H_4]^+$.
Anal. Calcd. for $C_{26}H_{36}N_2O_{10}$ 1.92 HCl (+0.45 H_2O): C, 50.80; H, 6.36; N, 4.55; O, 27.20; Cl, 11.07. Found: C, 50.79, H, 6.34; N, 4.53; O, 27.16, Cl, 11.05.

N,N′-BIS-(3,4,5-TRIMETHOXYBENZYL)ETHYLENEDIAMINE N,N′-DIACETIC ACID DIMETHYL ESTER. 10.0 g (20.3 mmoles) of N,N′-bis-(3,4,5-trimethoxybenzyl) ethylenediamine dihydrochloride was dissolved in 100 mL of DMF containing 40.6 mmoles triethylamine. Methyl bromoacetate (80.0 mmoles) and 40.0 mmoles calcium carbonate were then added and the mixture stirred at 80°C for 4 hr. The solution was evaporated to dryness under reduced pressure and then extracted with dichloromethane. The organic phase was washed with water, dried, and evaporated to dryness. The oily residue was purified by chromatography on silica gel to yield 3.40 g (30%) of N,N′-bis-(3,4,5-trimethoxybenzyl)ethylenediamine N,-N′-diacetic acid dimethyl ester as a white powder m.p. = 80°C.
^1H NMR (in $CDCl_3$): δ (ppm) = 2.69 (s, 4H), 3.40 (s, 4H), 3.59 (s, 6H), 3.62 (s, 6H), 3.65 (s, 4H), 3.70 (s, 12H), 6.59 (s, 4H).
MS (DCI, ammonia): m/z (% relative abundance): 565 (80), $[M + H]^+$; 181 (100), $[(MeO)_3\text{-}C_7H_4]^+$.
Anal. Calcd. for $C_{28}H_{40}N_2O_{10}$: C, 59.56; H, 7.14; N, 4.96; O, 28.34. Found: C, 59.29; H, 7.09; N, 4.90; O, 28.35.

Methods

HPLC ANALYSIS. HPLC analysis of Fe(III) OR10141 oxidation products was performed using a Waters Pursil 5 μm C18 120 Å column (15 cm × 4.6 mm) with a mobile phase containing 25% methanol, 2.6% isopropanol, 72.4% 10 mM pH 7.8 phosphate buffer, and 0.1 mM EDTA, at a flow rate of 1 mL/min. Chromatograms were recorded at 210 nm. Under the conditions used, ascorbate and EDTA were eluted in the dead volume. Under typical experimental conditions, chelate was incubated at room temperature with H_2O_2 and/or ascorbate for 1 hr. Iron was then dissociated from ligands by addition of 3 mM EDTA and heated at 40°C for 40 min.

MASS SPECTROMETRY AND NMR IDENTIFICATION OF OXIDATION PRODUCTS. OR10141 oxidation products were detected as ligands marked 1 to 4 in Fig. 4, using HPLC/ESI/MS with a mobile phase containing 17% methanol, 3% isopropanol, and 80% 10 mM ammonium acetate buffer at pH 7.

The main oxidation product 1 was also isolated as an iron chelate according to the following procedure. 1 mM ferric OR10141 chelate (prepared from ferric chloride) was incubated with 3 equivalents H_2O_2 in 10 mM ammonium acetate pH 7 for 1 hr. The resulting purple solution was first washed with dichloromethane and then saturated with NaCl to allow further extraction with dichloromethane. The resulting deep blue-purple organic phase was dried over magnesium sulfate and evaporated to dryness. This product was then analysed by ESI/MS (loop injection) for molecular weight determination (Table 1).

To run ^1H and ^{13}C NMR analysis on this product, which is intensely paramagnetic, it was solubilised in D_2O to which sodium dithionite was added. This induces an instantaneous bleaching of the purple solution and allows a restitution of NMR fine structure, presumably by reducing paramagnetic high spin ferric iron to diamagnetic ferrous iron. 2D spectrum analysis confirmed compound 1 structure as N-(2-hydroxy 3,4,5-trimethoxybenzyl) N′-(3,4,5-trimethoxybenzyl) ethylenediamine N,N′-diacetic acid (OR10163).

PROTECTION BY OR10141 AGAINST OXIDATIVE DAMAGE. DNA: Analysis of *in vitro* DNA single strand breaks was performed according to classical procedures [28, 29]. Supercoiled DNA (10 μg/mL) from pBR322 (Boehringer) in 10 mM aerated phosphate buffer pH 6.8 was incubated for 1 hr at 37°C with various concentrations of chelators and ascorbate (see Fig. legends). The buffer was pretreated with chelex 100 (Sigma) to remove adventitious traces of metals and the pH was readjusted. Reactions were performed in a final volume of 20 μL and stopped by addition of 10 μL of stop solution (4M urea, 50% sucrose, 50mM EDTA, 0.1% bromophenol blue). Samples were analysed by electrophoresis in 1% agarose gel in 89 mM tris borate 2 mM EDTA buffer. The gel was stained with ethidium bromide. Untreated plasmid DNA revealed a major band corresponding to the intact supercoiled form and a minor band corresponding to the nicked circular form.

Proteins: Protection of G-6-PDH against inactivation by Fenton reaction was measured according to [30]. Briefly, 5 μg/mL G-6-PDH (Boehringer, from yeast) was incubated for 1 min at 37°C in 10 mM MOPS and 100 mM KCl buffer with various concentration of OR10141. 50 μM $Fe(NH_4)_2(SO_4)_2$ were then added followed by 50 μM hydrogen peroxide and the mixture incubated for 5 min at 37°C. Residual activity was then determined by following the appearance of NADPH spectrophotometrically at 340 nm after addition of 150 μL aliquot of 10 mM $NADP^+$ and 100 mM glucose 6-phosphate to 2.85 mL of the enzyme solution.

Protein carbonyl content after incubation with iron and ascorbate was determined using 2,4-dinitrophenylhydrazine [30, 31]. The inactivation was carried out at 37°C for 30 min in open tubes containing the protein (1 mg/mL) in 10 mM phosphate buffer saline pH 7.4 to which were added various concentrations of chelators, 10 μM $FeCl_3$, 2 mM sodium ascorbate, and 2 mM hydrogen peroxide. Aliquots (2 mL) were precipitated with equal volumes of 20% TCA. One sample was treated with 2 mL of 2N HCl and the other with 2 mL of 0.2% 2,4-dinitrophenylhydrazine in 2N HCl. Both samples were incubated at 37°C for 2 hr. The samples were then reprecipitated with 2 mL of 20% TCA and washed twice with 3 mL of ethanol. The pellets were dissolved in 2 mL of 6M guanidine HCl. The absorption spectra (350–550 nm) were recorded against guanidine HCl and the amount of protein carbonyls estimated, using an average molar absorptivity of 22,000 at 370 nm. All experiments were performed in triplicate.

Lipid Peroxidation: Peroxidation of rat liver microsomes was measured by the TBA test [32]. Reaction mixtures contained, in 1 mL of 10 mM phosphate buffer saline pH 7.4: 0.44 mg/mL

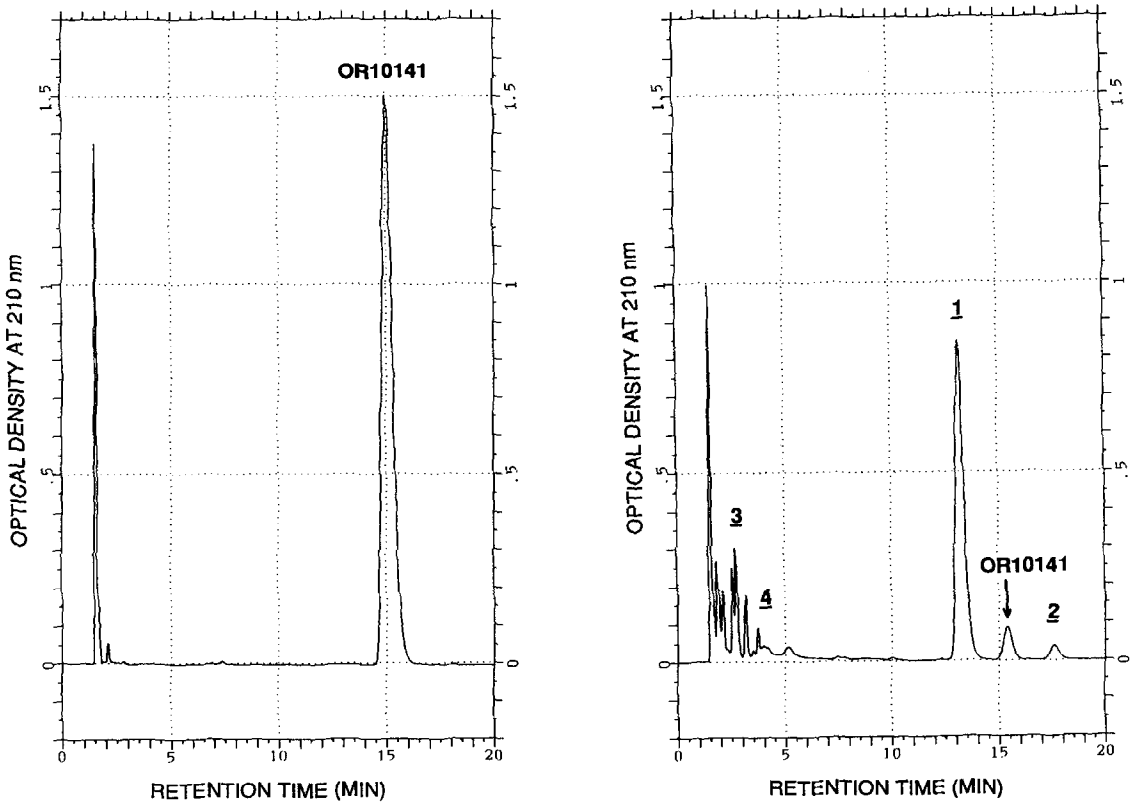

FIG. 4. HPLC chromatogram showing partial conversion of OR10141 to OR10163 (UV detection at 210 nm). 1 mM Fe(III)-OR10141 in 10 mM ammonium acetate buffer pH 7 was incubated at room temperature with hydrogen peroxide. After 1 hr incubation, EDTA (3 mM) was added to the solution and the mixture was heated for 40 min at 40°C to displace iron from the chelates before injection. (A) control without hydrogen peroxide; (B) oxidation with 3 mM hydrogen peroxide for 1 hr.

microsomal protein, $FeCl_3$ (10 μM), chelator (100 μM), and sodium ascorbate (1 mM). Solutions were stirred at 37°C in open tubes for 2 hr. Peroxidation was then measured in each sample by adding 0.5 mL 1% TBA in 0.05M NaOH and 0.5 ml 2.8% trichloroacetic acid and then heating for 15 min at 100°C. The pink chromophore was extracted in 2 mL butanol and the absorbance of the organic layer measured at 532 nm. Experiments were performed in triplicate.

Protection of Cultured Cells: Protection afforded by OR10141 in cultured cells submitted to hydrogen peroxide was evaluated by continuously following the physiological state of cells using a Cytosensor. The Cytosensor is a light potentiometric sensor-based device that detects changes in the rate of extracellular acidification of cultured living cells [33]. It may be used as an *in vitro* method for noninvasive and real time measurement of cell metabolism. Experiments were performed on epithelial cell line NCTC 2544 (ICN Laboratories). They were passaged in DMEM containing foetal calf serum (10%), penicillin/streptomycin (100 IU/mL, 100 μg/mL) and 1 mM L-glutamine. Cells were seeded on polycarbonate membrane insert (Transwell, 3 μm pore size) at a density of 3.10^5 cells per cm^2. Cells were introduced into the measurement chamber 24 hr later, and allowed to perfuse with a DMEM lacking fetal calf serum and bicarbonate (low buffer medium). Baseline metabolic rates were obtained during a control period. Cells were then treated with the chelator for 1 hr before glucose glucose oxidase (1 IU/mL and 25 mM, respectively) introduction at a constant flow rate (100 μL/min) for a period of 2 hr, during which the metabolic rate was measured every minute.

RESULTS AND DISCUSSION

Reactivity of OR10141 Iron Chelate with Hydrogen Peroxide

Incubation of ferric OR10141 complex, which is yellow, with excess ascorbate and hydrogen peroxide results in the instantaneous appearance of a strong purple chromophore with λ_{max} = 560 nm at pH 5.4 (Fig. 3a). The same chromophore also appears, although more slowly, in the absence of ascorbate (Fig. 3b). This intense visible band, whose λ_{max} varies with pH, is likely to be assigned to a charge transfer band from a π orbital on the phenolate ligand to a half-filled *d* orbital of iron [34]. The appearance of the 560 nm chromophore is apparently not significantly affected by visible light (not shown), but some photoreduction cannot be excluded because chemically-related structures [35] have been reported to be photoreducible. However, oxidation by hydrogen peroxide is likely to be a much faster reaction.

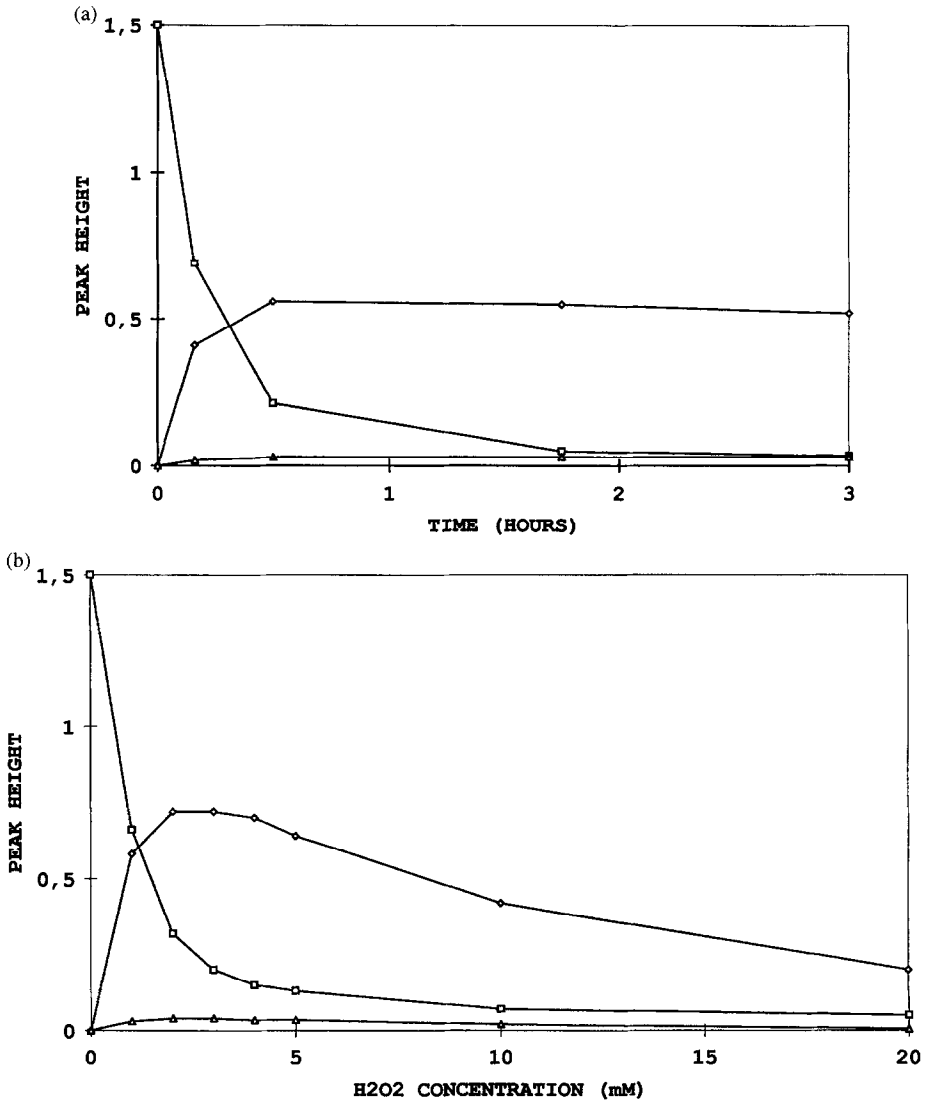

FIG. 5. (A) Evolution of OR10141, compound 1 and 2 HPLC peak height as a function of incubation time with 3 mM H_2O_2 of a 1 mM Fe(III)-OR10141 solution in 10 mM ammonium acetate buffer pH 7 at room temperature. After incubation time, EDTA (3 mM) was added to the solution and the mixture heated for 40 min at 40°C to displace iron from the chelates before injection. (B) Evolution of OR10141, compound 1 and 2 HPLC peak height as a function of hydrogen peroxide concentration after 1-hr incubation at room temperature of a 1 mM Fe(III)-OR10141 solution in 10 mM ammonium acetate buffer pH 7. After incubation time, EDTA (3 mM) was added to the solution and the mixture heated for 40 min at 40°C to displace iron from the chelates before injection. OR10141 (diamond), compound 1 (square), compound 2 (triangle).

The composition of this crude purple solution was analysed by HPLC and mass spectrometry. HPLC chromatograms obtained by injecting a crude purple solution show a significant unresolved large peak (not shown). On the other hand, when iron is displaced from chelates before injection by adding excess EDTA and heating for 40 min at 40°C, a good resolution is observed for the free ligands (Fig. 4) showing the apparition of one main product (compound 1) and a few minor ones.

TABLE 2. Mass spectrometry (MS) data permitting identification of compounds 2, 3, and 4 as structures proposed in Fig. 6

Compound N°	m/z (% relative abundance) $[M + Na]^+$	m/z (% relative abundance) $[M + H]^+$	m/z (% relative abundance) $[(MeO)_3 - C_7H_4]^+$
2	219 (60)	197 (100)	–
3	379 (15)	357 (100)	181 (15)
4	278 (100)	256 (15)	–

Analysis of 2, 3 and 4 were performed by HPLC/ESI/MS of an EDTA decomplexed mixture of ferric OR10141 oxidation products (see Materials and Methods).

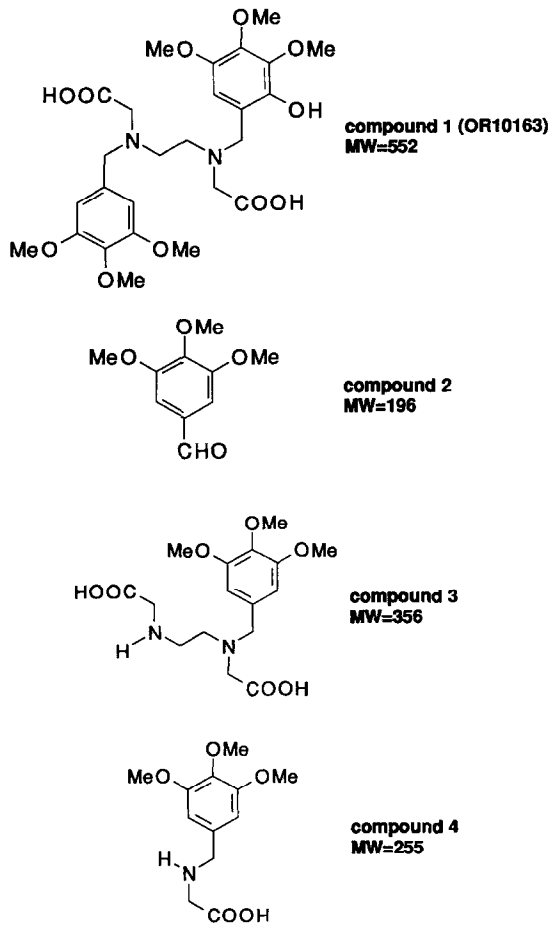

FIG. 6. Proposed structures of oxidation products of OR10141 detected by mass spectrometry.

Similar profiles are obtained for the reaction between Fe(III)-OR10141 and H_2O_2, either in the presence or in the absence of ascorbate (not shown).

Figure 5a and b, respectively show the evolution of peak height with time and hydrogen peroxide concentration for OR10141, compound 1 and compound 2 starting from 1 mM ferric OR10141 chelate in 10 mM pH 7 ammonium acetate buffer.

It is apparent that OR10141 is consumed during the time course of the reaction and is transformed mostly into compound 1. The latter was tentatively identified by HPLC/ESI/MS (Table 1) as N-(2-hydroxy 3,4,5-trimethoxybenzyl) N'-(3,4,5-trimethoxybenzyl) ethylenediamine N,N'-diacetic acid (OR10163, Fig. 1).

The structure of compound 1 iron as iron chelate was confirmed by mass spectrometry and by two dimension ^1H-^{13}C NMR (Table 1, see Material and Methods for details of isolation). This compound is, indeed, a pentadentate ligand with a phenol moiety that can coordinate iron as depicted in Fig. 2.

It can be seen from Fig. 5b that OR10163 yield decreases when more than 3 or 4 molar equivalents of hydrogen peroxide are incubated with ferric OR10141 chelate. However, OR10163 chelate destruction by excess oxidant occurs mainly during incubation with EDTA before HPLC injection. Indeed, comparable visible spectra are obtained by incubating OR10141 iron chelate either with 3 or 10 equivalents hydrogen peroxide (Fig. 3), which suggests that OR10163 chelate is stable even in the presence of more than 3 molar equivalents of hydrogen peroxide.

Figure 6 shows the structural propositions for some of the other oxidation products detected during the HPLC/ESI/MS of the EDTA-decomplexed mixture. These propositions were given following the interpretation of mass spectra as summarized in Table 2. Among them is 3,4,5-trimethoxybenzaldehyde (compound 2) and the corresponding scission molecule 3.

The maximum yield of 2 was estimated to be 6% by comparison with an authentic sample of pure 3,4,5-trimethoxybenzaldehyde. Owing to its probable mechanism of formation (see below) it may be concluded that the same amount of 3 is formed.

On the other hand, the yield of OR10163 formed after 1 hr reaction with 3 equivalents hydrogen peroxide is more than 80%, as estimated from both HPLC peak height using isolated ferric OR10163 chelate as a standard and colorimetric determination using a measured extinction coefficient of 1500 at 560 nm.

Moreover, Fig. 5b shows that more than 80% of OR10141 is consumed after 1 hr reaction with 2 equivalents of hydrogen peroxide, thereby indicating a very efficient oxidation pathway.

The extractibility of ferric OR10163 chelate by dichloromethane (see Material and Methods) suggests that the species is uncharged (i.e. that the sixth coordination site is occupied by a neutral ligand, for instance one water molecule) (see Fig. 2, X = H_2O). However, it is noteworthy that other purple species present in crude oxidation solution are not extractible by dichloromethane. These species could correspond to ferric OR10163 chelate bearing another sixth coordination site ligand, for example chloride or even a μ-oxo dimer. The overall charge would, therefore, be negative and, the species would thus, not be extractible by dichloromethane.

To summarize, these results show that OR10141 can be site-specifically oxidised in a similar way to that recently described for DBED [26], but that it is characterised by a higher reactivity towards intramolecular o-hydroxylation of the aromatic moiety.

Indeed, in this previous study, it was shown that monohydroxylated compound HBBED was one of the oxidation products. However, HBBED yield was low (10–15%) and various unidentified side products were formed, likely resulting from further hydroxylation of the aromatic rings.

In the case of OR10141, both the appearance of 560 nm chromophore and HPLC analysis show that conversion to OR10163 is much higher than conversion of DBED to HBBED. Moreover, stoichiometry of hydrogen peroxide is much lower than in the case of DBED. Increased electron density in position 2 of the aromatic rings due to methoxy substituants in positions 3 and 5 is likely to be responsible for the high oxidation yield because it favors electrophilic addition of hydroxyl radical and also prevents HO· addition in these positions.

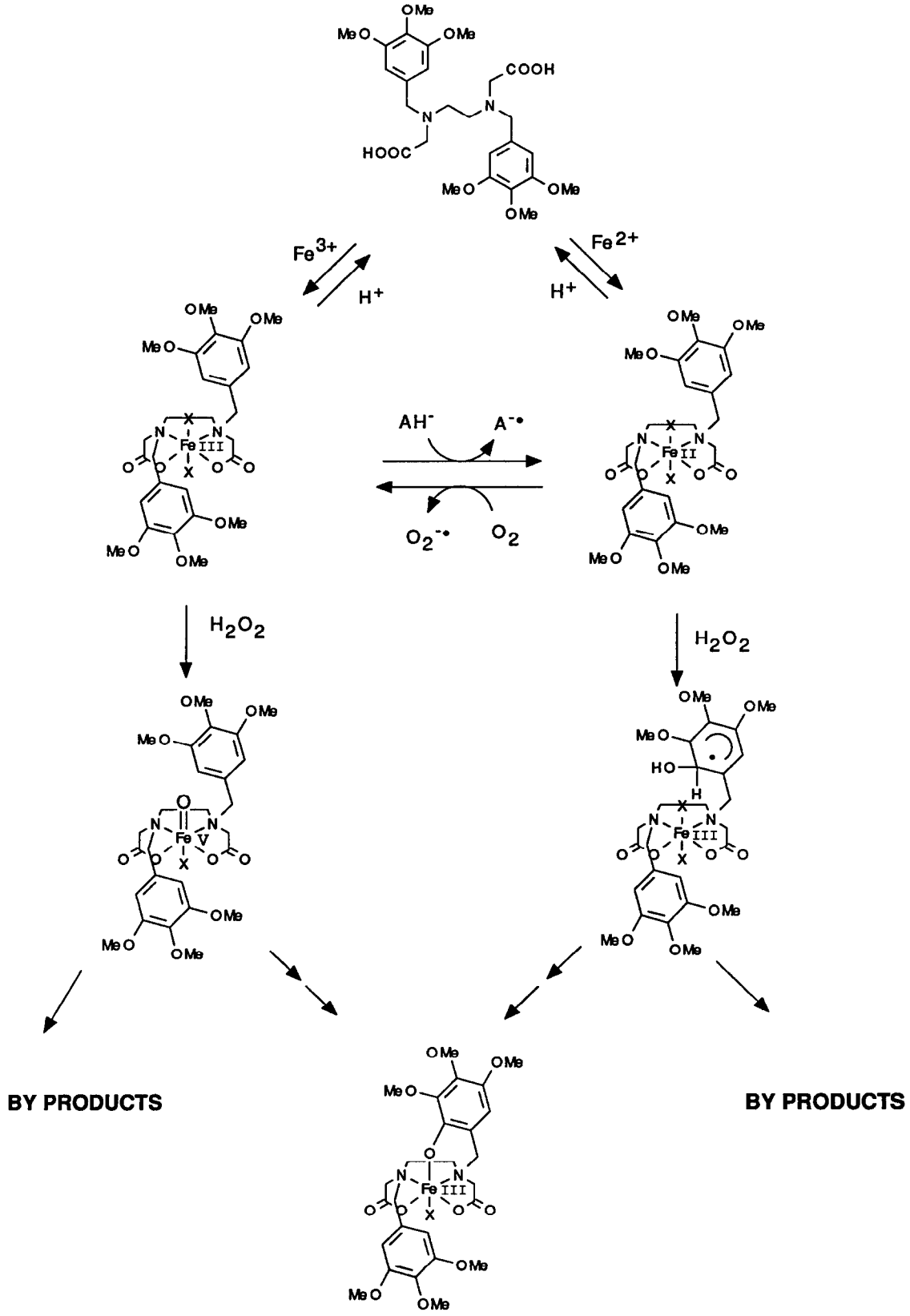

FIG. 7. Proposed scheme showing reaction between OR10141, iron, hydrogen peroxide, and ascorbate (AH^-); X represents axial ligand.

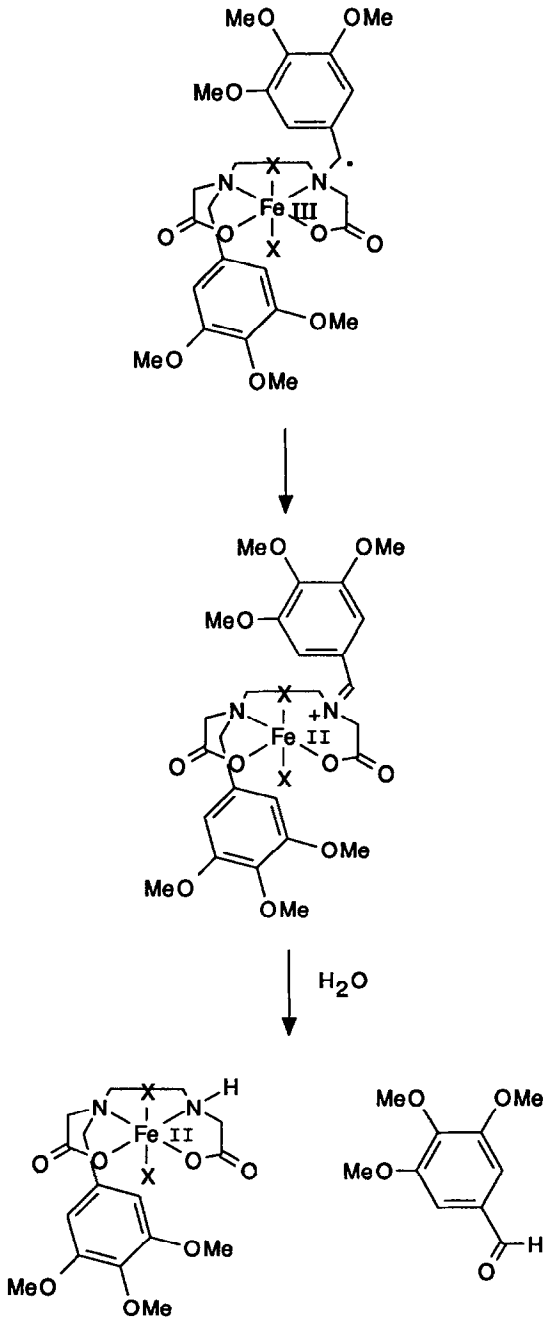

FIG. 8. Proposed mechanism for 3,4,5 trimethoxy benzaldehyde formation.

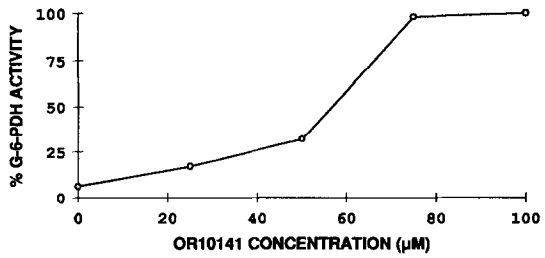

FIG. 9. Protection by OR10141 against loss of G-6PDH activity induced by Fenton reaction. Enzyme at a concentration of 5 μg/mL was incubated for 1 min at 37°C in 10 mM MOPS and 100 mM KCl in the presence of the concentration of OR10141 indicated on the abscissa. 50 μM Fe(II) and 50 μM H_2O_2 were then added and the remaining activity after 5-min incubation was assayed as described in Materials and Methods and expressed as % of untreated enzyme.

Possible Mechanisms of Reaction between OR10141 Iron Chelate and Hydrogen Peroxide

A mechanisms is proposed in Fig. 7 that tentatively takes into account reactions of hydrogen peroxide with both ferric and ferrous OR10141 chelate. Owing to structural features, hydroxylation of position 2 of the benzyl moieties is highly sterically favoured. Reaction of ferrous complex is likely to involve an $HO^{\cdot}$ (or, alternatively, an $Fe^{IV} = O$ ferryl-type species) which, when added to the aromatic moiety, would lead to a HCHD intermediate. Because electron-rich HCHD are known as powerful one-electron reductants [36], it can be speculated that it will reduce Fe(III) leading to a ferrous chelate that could react with a second H_2O_2 molecule. Therefore, a secondary $HO^{\cdot}$ could be formed and induce radical damage to surrounding molecules under physiological conditions. However, this damage should be weak compared to the potential multiple oxidative damage that would have been catalysed by iron in the absence of OR10141.

Reaction between ferric OR10141 chelate and hydrogen peroxide likely involves an $Fe^{V} = O$ oxo-type species leading to the same final monohydroxylation product. Reduction of iron by H_2O_2 leading to $O_2^{-\cdot}$ is also possible, already having been observed for iron EDTA chelate [21].

In the presence of ascorbate, reduction of Fe(III) seems to be much faster than the reaction between ferric chelate and H_2O_2. On the other hand, autoxidation of ferrous OR10141 is much slower than reaction with hydrogen peroxide (not shown).

Formation of small amounts of compounds 2, 3, and 4 described in Fig. 6 may derive from α-amino hydrogen abstraction by hydroxyl radical followed by an electron transfer leading to an imminium cation as shown in Fig. 8 in the case of benzylic hydrogen (see, for instance [37, 38]). In this particular case, 3,4,5-trimethoxybenzaldehyde and the corresponding moiety 3 are formed. Detection of compound 4 shows that hydrogen abstraction from ethylenediamine link also occurs.

Implications of "Oxidative Activation"

The affinity constant of Fe(III) for OR10141 was evaluated potentiometrically to be log K < 15 according to classical methods [39] (μ = 0.1M KNO_3). For calculation of the overall equilibrium constant, ligand pKa values were measured from potentiometric titration to be 4.8 and 9.6.

Because the affinity of OR10141 for iron is low, it may be hoped that iron mobilisation from metalloproteins will be avoided and, therefore, that the adverse side effects related to "safe" iron chelation will be low. As a comparison, affinity of ferric iron for transferrin is log K = 21 [40]. Therefore,

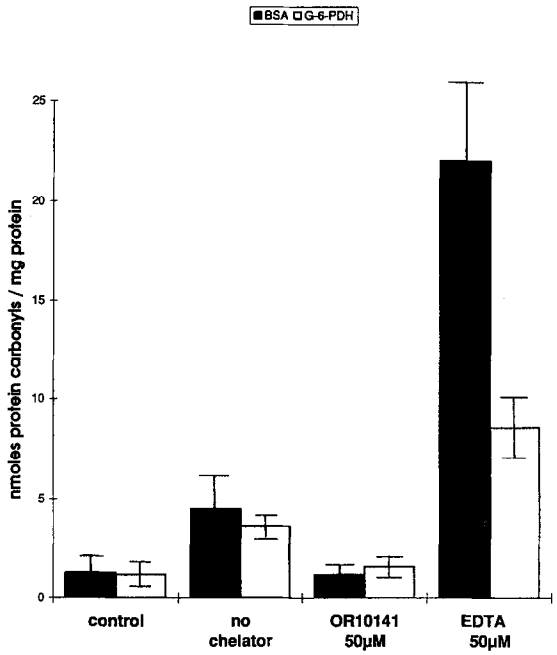

FIG. 10. Protein carbonyl content after 30-min incubation of BSA and G-6-PDH with 10 µM $FeCl_3$, 2 mM ascorbate, and 2 mM H_2O_2 and 50 µM chelators in 10 mM phosphate buffer pH 7.4 at 37°C. Protein carbonyls were determined using 2,4-dinitrophenylhydrazine as described in Materials and Methods.

OR10141 cannot compete for iron of transferrin thermodynamically.

On the other hand, the affinity of OR10163 for Fe(III) was estimated to be in the range of that of HBBED [26] (e.g. log K # 28). Moreover, it was found (not shown), as for HBBED, that although Fe(III) OR10163 still has one uncoordinated site it is not a catalyst of Fenton chemistry, probably because of a decrease in redox potential of iron that is likely to prevent further iron reduction.

Therefore, it can be hypothesized that, under oxidative stress conditions *in vivo*, OR10141 could decrease free iron availability and catalytic properties by the above-described site-specific oxidation and, thus, protect a tissue against oxidative stress.

TABLE 3. Protection by OR10141 against iron ascorbate-induced microsomal lipid peroxidation

Additions	Amount of TBARs (A^{532})
None	0.16 ± 0.03
$FeCl_3$/Asc.	1.19 ± 0.04
$FeCl_3$/Asc./OR10141	0.09 ± 0.01
$FeCl_3$/Asc./Desferal	0.09 ± 0.01
$FeCl_3$/Asc./EDDA	1.20 ± 0.03

Rat liver microsomes (0.44 mg protein/mL) were incubated for 2 hr at 37°C in aerated 10 mM phosphate buffer saline pH 7.4 with or without the following additions: chelator (100 µM), $FeCl_3$ (10 µM), and sodium ascorbate (Asc., 1 mM). Peroxidation was measured as TBARs as described in Materials and Methods. Values are the means ± SD of triplicate experiments.

It seems that such a benefit can reasonably be expected from the following results showing protective effects by OR10141 against oxidative damage to biological molecules *in vitro*.

Protective Effects against Oxidative Damage in vitro

When added to a protein in the presence of an iron-dependent hydroxyl radical generating system, OR10141 effectively inhibited protein damage. This is illustrated both in Fig. 9 and Fig. 10, which show OR10141 protective against inactivation of G-6-PDH by Fenton reaction and formation of protein carbonyl on BSA and G-6-PDH by the iron ascorbate system, respectively. In both systems, OR10141 protection is effective at concentrations slightly above iron concentration.

The effects of OR10141 were also investigated in experiments based on the relaxation and linearisation of supercoiled DNA, which is a very sensitive measurement of single-strand breaks in DNA (Fig. 11). Incubation of 10 µg/mL DNA and 1 mM ascorbate in the presence of increasing concentrations of $FeCl_3$ in aerated phosphate buffer induced a dose-dependent appearance of strand breaks after 1 hr at 37°C. The effect of various chelators was evaluated in the assay. EDDA at 100 µM dramatically increased the damage produced by iron and ascorbate, supercoiled DNA being almost quantitatively linearised (not shown). On the other hand, 100 µM or 1 mM OR10141 inhibited DNA damage induced by submicromolar concentrations of iron. Protection afforded by OR10141 is comparable to that obtained with deferoxamine mesylate and HBED (not shown). Protection by OR10141 is not so efficient for higher concentrations of iron (i.e. 5 and 10 µM).

Inhibition by OR10141 of iron ascorbate-induced rat liver microsome lipid peroxidation was also demonstrated (Table 3). OR10141 is as effective as DF mesylate and totally inhibits peroxidation catalysed by 10 µM $FeCl_3$ under our conditions. Conversely, EDDA does not offer any protection.

Protective effects of OR10141 were, finally, evaluated against deleterious effects induced by hydrogen peroxide using a Cytosensor (see Material and Methods). Metabolic acidification of an epithelial cell line (NCTC 2544) was continuously monitored to determine noninvasively the effects of hydrogen peroxide generated by glucose glucose oxidase. Hydrogen peroxide induced a decline in metabolic rate. Pretreatment of cells with DF mesylate, o-phenantroline, and HBED significantly reduced the decrease in metabolic rate (Fig. 12). On the other hand, OR10141 did not significantly protect cells even at high concentrations. Therefore, because membrane permeability of OR10141 is assumed to be poor, we decided to investigate the effect of dimethyl ester of OR10141 as a prodrug of the chelator which could be cleaved by membrane nonspecific esterases. Indeed, in the case of fluorescent calcium chelator Quin2, cell loading by means of intracellularly hydrolyzable esters has been demonstrated [41]. Hence, a significant protection by OR10141 ester was observed. However, relatively high concentrations are still needed (limited by water solubility, e.g. 1 mM), which suggests that OR10141 bioavailability is poor even as a prodrug ester. This might be related to a low rate of cellular hydrolysis. However, protection

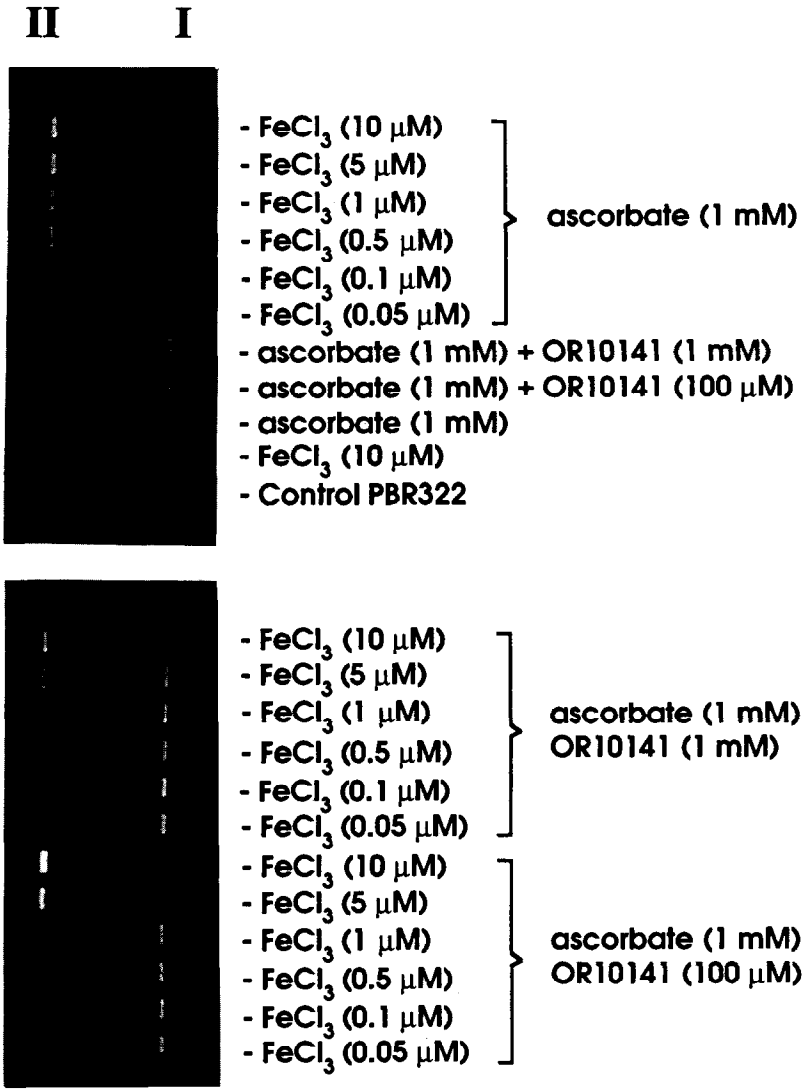

FIG. 11. Iron chelate-mediated production of DNA strand breaks. Supercoiled plasmid DNA was incubated with various concentrations of $FeCl_3$, 100 µM or 1 mM chelator, and 1 mM sodium ascorbate for 1 hr at 37°C in 10 mM phosphate buffer pH 6.8 as described in Materials and Methods. I and II indicate the positions of migrated supercoiled and circular forms of plasmid DNA, respectively.

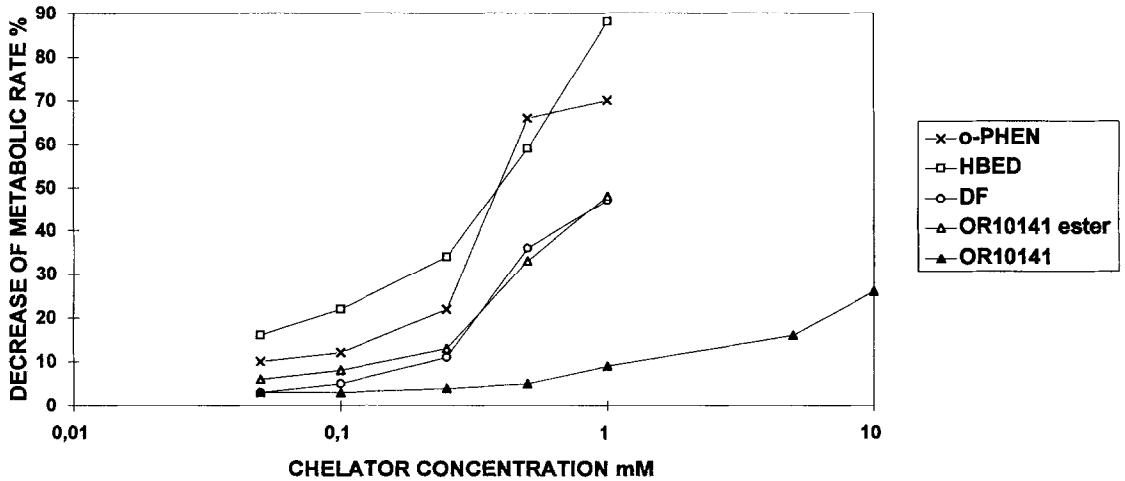

FIG. 12. Protection afforded by OR10141 and its dimethyl ester on cultured cells submitted to a flux of H_2O_2 generated from glucose glucose oxidase. Deleterious effects of hydrogen peroxide were measured by the decrease in metabolic rate using a Cytosensor as described in Materials and Methods. The NCTC 2544 cell line was treated with various concentrations of chelators for 1 hr before addition of 25 mM glucose and 1 U/mL glucose oxidase for 2 hr, during which the metabolic rate was measured every minute. The graph shows results at the end of the 2-hr period. Metabolic rates are expressed in % comparatively to control values of untreated cells. o-PHEN is o-phenantroline, HBED is N,N'-bis-(2-hydroxybenzyl) ethylenediamine N,N'-diacetic acid and DF is deferoxamine mesylate.

efficiency in this assay is comparable to that afforded by deferoxamine, which is known to have poor membrane permeability.

On the other hand, neither OR10141 nor its dimethyl ester up to 1 mM is able to protect cells against hydrogen peroxyde cytotoxicity in CHO cells as measured by a cloning efficiency assay.* This result suggests that the amount of OR10141 that enters the cell might not be enough to reach certain critical targets, for instance the nucleus, where reactions with radical species can lead to cell death.

However, the positive results obtained by measuring the decrease in metabolic rate induced by a low flux of hydrogen peroxide generated by glucose glucose oxidase suggest that the compound is able to reach other targets, at least those involved in metabolic function. Indeed, one of the earliest targets of the hydrogen peroxide deleterious effect has been described as some enzymes of energetic metabolism [42].

Potential Biological Applications

Our results show that in pure *in vitro* systems, OR10141 is able to protect each class of biological molecule: proteins, lipids, and DNA, against iron-catalysed oxidative damage. This suggests that the affinity for iron of OR10141 is high enough to partially withdraw nonspecifically bound iron from target molecules. Secondary to weakly-bound iron displacement by OR10141, it is tempting to speculate that protection is more probably the result of strong iron chelation by oxidized ligand than of hydroxyl radical scavenging. Indeed, a good protection could hardly be anticipated from scavenging a unique $HO^{\cdot}$ compared to H_2O_2 excess.

However, further work will be necessary to elucidate the protective mechanism.

Results of experiments in cellular systems are more disappointing. The poor efficiency of OR10141 in cellular assays is likely the result of its inability to cross cell membrane. Indeed, it has been reported by others that hydrophilic iron chelators, such as DTPA, do not protect cells against the deleterious effects of hydrogen peroxide because they do not reach intracellular iron [17, 43]. These results could signify that potential applications of OR10141 could be restricted to extracellular iron chelation. OR10141 could, for instance, have some relevance against chronic exposure to UV light, which has been shown to result in an increased level of non-heme iron. This iron accumulation may be the result of UVB irradiation-induced capillary damage and leakage of protein-bound iron [44].

However, vectorization of OR10141, or synthesis of other prodrugs may also favour membrane penetration and, therefore, allow the chelator to reach a sufficient intracellular concentration so as to afford protection against iron-catalysed oxidative damage.

In conclusion, it must be emphasized that, contrary to strong iron chelator, the relatively low affinity of OR10141 for iron may very well prevent interference with iron metabolism and, therefore, the use of OR10141 and related prodrugs in chronic situations in which treatment for prolonged periods of time is required could be feasible. Potential medicinal applications of OR10141 and related prodrugs could, therefore, concern pharmacological treatment of a variety of diseases where a continuous production of reduced oxygen species is suspected. These situations include inflammatory diseases [3, 23], atherosclerosis [22], iron overload [45], neurodegenerative diseases [46–48], and protection against toxicity of redox cycling drugs [49].

The authors thank Prof. Marc Fontecave for stimulating discussions and helpful comments on the manuscript.

* Prof. O. Cantoni, private communication cited with permission.

References

1. Halliwell B and Gutteridge JMC, *Free Radicals in Biology and Medicine*, second Ed. Clarendon Press, Oxford, 1989.
2. Sies H, Biochemistry of oxidative stress. *Angew Chem Int Ed Engl* **25:** 1058–1071, 1986.
3. Trenam CW, Blake DR and Morris CJ, Skin inflammation: reactive oxygen species and the role of iron. *J Invest Dermatol* **99:** 675–682, 1992.
4. Fuchs J and Packer L, *Oxidative Stress in Dermatology*. Marcel Dekker Inc., New York, Basel, Hong Kong, 1993.
5. Ames BN and Shigenaga MK, Oxidants are a major contributor to aging. *Ann NY Acad Sci* **663:** 85–96, 1992.
6. Harman D, The aging process. *Proc Natl Acad Sci USA* **78** (11): 7124–7128, 1981.
7. Chance B, Sies H and Boveris A, Hydroperoxide metabolism in mammalian organs. *Physiol Rev* **59**(3): 527–605, 1979.
8. Halliwell B, Gutteridge JMC and Cross CE, Free radicals, antioxidants, and human disease: Where are we now? *J Lab Clin Med* **119**(6): 598–620, 1992.
9. Fontecave M and Pierre J-L, Iron: metabolism, toxicity and therapy. *Biochimie* **75:** 767–73, 1993.
10. Klausner RD, Rouault TA and Harford JB, Regulating the fate of mRNA: the control of cellular iron metabolism. *Cell* **72:** 19–28, 1993.
11. Ryan TP and Aust SD, The role of iron in oxygen-mediated toxicities. *Crit Rev Toxicol* **22**(1): 119–141, 1992.
12. Miller DM, Buettner GR and Aust SD, Transition metals as catalysts of "autoxidation" reactions. *Free Rad Biol Med* **8:** 95–108, 1990.
13. Chevion M, A site-specific mechanism for free radical induced biological damage: the essential role of redox-active transition metals. *Free Rad Biol Med* **5:** 27–37, 1988.
14. Stadtman ER, Metal ion-catalysed oxidation of proteins: biochemical mechanism and biological consequences. *Free Rad Biol Med* **9:** 315–325, 1990.
15. Imlay JA, Chin SM and Linn S, Toxic DNA damage by hydrogen peroxide through the Fenton reaction *in vivo* and *in vitro*. *Science* **240:** 640–642, 1988.
16. Tachon P, Ferric and cupric ions requirement for DNA single-strand breakage by H_2O_2, *Free Rad Res Commun* **7:** 1–10, 1989.
17. Burkitt MJ, Milne L, Tsang SY and Tam SC, Calcium indicator dye Quin2 inhibits hydrogen peroxide-induced DNA strand break formation via chelation of iron. *Arch Biochem Biophys* **311**(2): 321–328, 1994.
18. Dean RT and Nicholson P, The action of nine chelators on iron-dependent radical damage. *Free Rad Res* **20**(2): 83–101, 1994.
19. Tyrell R, UVA (320–380 nm) radiation as an oxidative stress. In:

Oxidative Stress, Oxidants and Antioxidants (Ed. Sies H), pp. 57–83. Academic Press Limited, San Diego 1991.
20. Graf E, Mahoney JR, Bryant R and Eaton JW, Iron-catalysed hydroxyl radical formation. Stringent requirement for free iron coordination site. *J Biol Chem* **259**(6): 3620–3624, 1984.
21. Gutteridge JMC, Superoxide-dependent formation of hydroxyl radicals from ferric-complexes and hydrogen peroxide: an evaluation of fourteen iron chelators. *Free Rad Res Comms* **9**(2): 119–125, 1990.
22. Voest EE, Vreugdenhil G and Marx JJM, Iron chelating agents in non-iron overload conditions. *Ann Intern Med* **120:** 490–499, 1994.
23. Polson RJ, Jawed A, Bomford A, Berry H and Williams R, Treatment of rheumatoid arthritis with desferrioxamine: relation between stores of iron before treatment and side effects. *Br Med J* **291:** 448, 1985.
24. Ganeshaguru K, Lally JM, Piga A, Hoffbrand AV and Kontoghiorghes GJ, Cytotoxic mechanisms of iron chelators. *Drugs Today* **28**(suppl. A): 29–34, 1992.
25. Porter JB and Huens ER, The toxic effects of desferrioxamine. *Bailliere's Clin Haematol* **2**(2): 459–474, 1989.
26. Galey J-B, Dumats J, Beck I, Fernandez B and Hocquaux M, N,N′-bis-dibenzyl ethylenediaminediacetic acid: a site specific hydroxyl radical scavenger acting as an "oxidative stress activatable iron chelator" in vitro. *Free Rad Res* **22**(1): 67–86, 1995.
27. Sun Y, Martell AM, Reibenspies JH and Welch MJ, Synthesis of multidentate ligands containing hydroxypyridyl donor groups. *Tetrahedron* **47**(3): 357–364, 1991.
28. Toyokuni S and Sagripanti JL, Iron-mediated DNA damage: sensitive detection of DNA strand breakage catalysed by iron. *J Inorganic Biochem* **47:** 241–248, 1992.
29. Marrot L and Giacomoni P, Enhancement of oxidative DNA degradation by histidine: the role of stereochemical parameters. *Mutation Res* **275:** 69–79, 1992.
30. Szweda LI and Stadtman ER, Iron-catalysed oxidative modification of glucose-6-phosphate Dehydrogenase from *Leuconostoc mesenteroides*. Structural and functional changes. *J Biol Chem* **267**(5): 3096–3100, 1992.
31. Hu ML and Tappel AL, Potentiation of oxidative damage to proteins by ultraviolet A and protection by antioxidants. *Photochem Photobiol* **56**(3): 357–363, 1992.
32. Aruoma OI, Evans PJ, Kaur H, Sutcliffe L and Halliwell B, An evaluation of the antioxidant and potential pro-oxidant properties of food additives and of trolox C, vitamin E and probucol. *Free Rad Res Commun* **10**(3): 143–157, 1990.
33. Mc Connel HM, Rice P, Wada GH, Owicki JC, Parce JW, The microphysiometer biosensor. *Curr Opin Structural Biol* **1:** 647–652, 1991.
34. Ramesh K and Mukherjee R, Trends in the spectral and redox potential data of mononuclear iron (III) (S = 5/2) phenolate complexes. *J Chem Soc Dalton Trans* 83–89, 1992.
35. Chao CC and Aust AE, Photochemical reduction of ferric iron by chelators results in DNA strand breaks. *Arch Biochem Biophys* **300**(2): 544–550, 1993.
36. Steenken S, Addition-elimination paths in electron-transfer reactions between radicals and molecules. *J Chem Soc Faraday Trans 1* **83:** 113–124, 1987.
37. Motekaitis R, Martell AE and Hayes D, The iron(III)-catalysed oxidation of EDTA in aqueous solution. *Can J Chem* **58**(19): 1999–2005, 1980.
38. Walling C and Johnson RA, Fenton's reagent. V. Hydroxylation and side chain cleavage of aromatics. *J Am Chem Soc* **97**(2): 363–367, 1975.
39. Chaberek Jr S and Martell AE, Stability of metal chelates. IV. N,N′-ethylenediaminediacetic acid and N,N′-ethylenediaminediacetic-N,N′-dipropionic acid. *J Am Chem Soc* **74:** 6228–6231, 1952.
40. Harris WR, Carrano CJ and Raymond KN, Coordination chemistry of microbial iron transport compounds. 16. Isolation, characterisation, and formation constants of ferric aerobactin. *J Am Chem Soc* **101**(10): 2722–2727, 1979.
41. Tsien R, Pozzan T and Rink TJ, Calcium homeostasis in intact lymphocytes: cytoplasmic free calcium monitored with a new, intracellularly trapped fluorescent indicator. *J Cell Biol* **94:** 325–334, 1982.
42. Hyslop PA, Hinshaw DB, Halsey Jr WA, Schraufstatter IU, Sauerheber RD, Spragg RG, Jackson JH and Cochrane CG, Mechanism of oxidant-mediated cell injury. The glycolytic and mitochondrial pathways of ADP phosphorylation are major intracellular targets inactivated by hydrogen peroxide. *J Biol Chem* **263:** 1665–1675, 1988.
43. Mello-Filho AC and Meneghini R, Iron is the intracellular metal involved in the production of DNA damage by oxygen radicals. *Mut Res* **251:** 109–113, 1991.
44. Bissett DL, Chatterjee R and Hannon DP, Chronic ultraviolet radiation-induced increase in skin iron and the photoprotective effect of topically applied iron chelators, *Photochem Photobiol* **54**(2): 215–223, 1991.
45. Hider RC and Singh S, Iron chelating agents with clinical potential. *Proc Roy Soc Edinburgh* **99B**(1/2): 137–168, 1992.
46. Gerlach M, Ben-Schachar D, Riederer P and Youdim MBH, Altered brain metabolism of iron as a cause of neurodegenerative diseases. *J Neurochem* **63**(3): 793–807, 1994.
47. Halliwell B, Reactive oxygen species and the central nervous system. *J Neurochem* **59:** 1609–1623, 1992.
48. Behl C, Davis JB, Lesley R and Schubert D, Hydrogen peroxide mediates amyloid β protein toxicity. *Cell* **77:** 817–827, 1994.
49. Hasinoff BB, Pharmacodynamics of the hydrolysis-activation of the cardioprotective agent (+)-1,2-bis(3,5-dioxopiperazin-1-yl)-propane. *J Pharm Sci* **83**(1): 64–67, 1994.